Vibrational Echo Studies of Myoglobin−CO

C. W. Rella,[†] K. D. Rector,[‡] Alfred Kwok,[‡] Jeffrey R. Hill,[§] H. A. Schwettman,[†] Dana D. Dlott,*[,§] and M. D. Fayer*[,‡]

Stanford Free Electron Laser Center, Hansen Experimental Physics Laboratory, Stanford University, Stanford, California 94305-4085, Department of Chemistry, Stanford University, Stanford, California 94305, and School of Chemical Sciences, University of Illinois at Urbana−Champaign, Urbana, Illinois 61801

Received: April 17, 1996; In Final Form: June 27, 1996[⊗]

The first picosecond infrared vibrational echo experiments on a protein, myoglobin−CO, are described. These vibrational dephasing experiments examine the influence of protein dynamics on the CO ligand bound to the active site of the protein at physiologically relevant temperatures. The experiments were performed with a mid-IR free electron laser tuned to the CO stretch mode at 1945 cm^{-1}. The vibrational echo results are combined with infrared pump−probe measurements of the CO vibrational lifetime to yield the homogenous pure dephasing, the Fourier transform of the homogeneous line width with the lifetime contribution removed. The measurements were made from 60 to 300 K. The results show that the CO vibrational spectrum is inhomogeneously broadened, even at room temperature. Above the glycerol/water solvent's glass transition temperature, ∼185 K, the temperature dependence can be fit as an activated process with $\Delta E \approx 1000$ cm^{-1}. Below 185 K, the pure dephasing displays a power law temperature dependence, $T^{1.3}$. This temperature dependence is reminiscent of that associated with the properties of low-temperature glasses (<5 K) but is observed at much higher temperatures. A two-level system model of protein dynamics is considered. The nature of the temperature dependence and the mechanism of the coupling of the protein fluctuations to the CO vibrational transition energy are discussed.

I. Introduction

In this paper, we present the first vibrational echo experiments performed on a protein. The vibrational echo is a time domain experiment that measures the Fourier transform of the homogeneous vibrational line shape.[1] By combining vibrational echo measurements with vibrational pump−probe lifetime measurements, the dynamical contributions to a vibrational transition can be elucidated.[1] Previous optical coherence experiments performed on proteins examined the dephasing of electronic transitions.[2] Because of the very rapid dephasing (broad homogeneous line widths) of electronic transitions, these experiments can only be performed at very low temperatures, i.e., a few degrees K. The vibrational echo experiments make it possible to use optical coherence methods to study protein dynamics at physiologically relevant temperatures.

From a vibrational absorption spectrum, it is not possible to determine if a line shape is inhomogeneously or homogeneously broadened. The vibrational echo makes the homogeneous line a direct experimental observable and, with lifetime measurements, permits the pure dephasing (energy level fluctuations) and the lifetime contributions to be separated. The experiments presented here were performed on the vibrational stretching mode of carbon monoxide (CO) bound to the active site of myoglobin (Mb).

Mb, a protein found in muscle tissue, is used in the storage and transport of dioxygen (O_2).[3] It consists of a prosthetic group called protoheme [iron(II) protoporphyrin IX] embedded in a protein shell. The protein modifies the chemical reactivity of the Fe binding site, allowing Mb to function properly in a biological setting.[3]

A substantial literature exists that explores the structure and binding kinetics of CO bound at the active site of Mb using a variety of techniques, including X-ray crystallography,[4] ^{13}C NMR,[5] time-dependent visible optical spectroscopy,[6] Raman spectroscopy,[7] and linear mid-IR spectroscopy.[8] Mid-IR spectroscopy of the CO stretching frequency has a demonstrated utility, supplying insights into how the structure of the protein modifies the nature of the binding site. When bound to Mb, the CO gas phase frequency is substantially red-shifted and separated into several distinct bands, which are labeled A_0-A_3 in order of decreasing carbonyl frequency. Although the intensity and widths of these bands are sensitive to temperature, mild pressure changes, and pH, their peak frequencies remain largely unchanged.

In general, methods such as IR spectroscopy and X-ray crystallography yield a wealth of information about the equilibrium structure of Mb−CO but can provide only indirect dynamical information. Room temperature proteins are dynamic. Molecular dynamics simulations of Mb suggest a flexible structure in constant motion rather than a rigid, scaffold-like structure.[9] Such motions can be on a relatively small scale involving few of the constituent Mb atoms, such as the torsion of an amino acid residue, or they can be large-scale motions involving entire regions of the protein backbone. Simulations over a period of 300 ps indicate that Mb samples thousands of local energy minima of approximately equal energy, separated by barriers of varying height.[9] These minima correspond to different conformational states of the protein. It has been proposed that this characteristic of proteins is analogous to the energy landscape in glasses.[10]

In this paper, a detailed temperature-dependent vibrational echo study of the CO stretching mode of Mb−CO is presented. The experiments were conducted using a free electron laser as the source of tunable picosecond IR pulses. In addition to the echo measurements, the temperature dependence of the vibra-

* Authors to whom correspondence should be addressed.
[†] Stanford Free Electron Laser Center.
[‡] Department of Chemistry, Stanford University.
[§] School of Chemical Sciences, University of Illinois at Urbana−Champaign.
[⊗] Abstract published in *Advance ACS Abstracts,* August 15, 1996.

S0022-3654(96)01129-X CCC: $12.00

tional lifetime was measured using IR pump−probe experiments. At the lowest temperature studied (60 K), the homogeneous line is dominated by the lifetime contribution (T_1), although the pure dephasing (T_2*) still makes a measurable contribution. At all temperatures, the vibrational echo decays are exponential. Thus, the homogeneous line is Lorentzian in shape. By room temperature, the homogeneous line width arises almost completely from pure dephasing. The homogenous line width (2.7 cm^{-1}) is substantially less than the width of the absorption spectrum (13.1 cm^{-1}), demonstrating that the line is inhomogeneously broadened, even at room temperature.

Above the glycerol/water solvent's glass transition (∼185 K), the liquid solvent provides a soft boundary condition for the protein motions. The protein can undergo large amplitude as well as small amplitude conformational changes. These changes in protein conformation couple to the CO bound to the active site and cause the CO vibrational energy levels to fluctuate, giving rise to pure dephasing. The data are well fit by an activated process with an activation energy on the order of 1000 cm^{-1}. This activation energy is associated with potential barrier heights for protein conformational changes.

Below 185 K, the temperature dependence of the pure dephasing line width ($1/\pi T_2$*) is a power law, $T^{1.3}$. This temperature dependence is the same as that observed for electronic excited state dephasing[11] and heat capacities[12] in very low temperature (<5 K) glasses, where a tunneling two-level system (TLS) model is used to explain the data.[13] However, this is the first time that a power law with such a small exponent has been observed for a pure dephasing process at such elevated temperatures. At higher temperatures (>10 K) in glasses, dephasing has either a T^2 or exponentially activated dependence on temperature, and heat capacities have a T^3 dependence. The observation of a $T^{1.3}$ dependence for vibrational dephasing of Mb−CO may suggest a tunneling TLS process for the protein. Protein dynamics dominated by tunneling can be shifted to higher temperature because of high energy barriers for conformational changes induced by the rigid boundary condition imposed by the glassy solvent. This possibility is discussed in terms of a protein two-level system (PTLS) model.

The nature of the coupling of the protein fluctuations to the CO vibrational transition energy is also addressed. A model is suggested in which protein fluctuations modulate the heme electron density, causing fluctuations in the back-bonding (back donation of electron density from the heme π electron system to the CO π* antibonding molecular orbital). Fluctuations in back-bonding give rise to energy level fluctuations and thus T_2*. Therefore, the vibrational echo experiments provide an observable for the communication of protein dynamics to a ligand bound to the active site of the protein.

II. The Vibrational Echo Method and Experimental Procedures

In disordered, condensed matter systems, in general, even a well-resolved vibrational line does not provide information on dynamics. Vibrational line shapes in condensed phases contain the details of the dynamic interactions of a normal mode with its environment.[14] However, the line shape can also include essentially static, structural perturbations associated with the distribution of local configurations of the environment, i.e., inhomogeneous broadening. The IR absorption or Raman line shape represents a convolution of the various dynamic and static contributions, and contributions from inhomogeneous broadening cannot be eliminated.[15]

The picosecond IR vibrational echo experiment is a time domain, nonlinear method that can extract the homogeneous vibrational line shape from inhomogeneously broadened lines.[1,16] The echo technique was originally developed as the spin echo in magnetic resonance in 1950.[17] In 1964, the method was extended to the visible optical regime as the photon echo.[18] Since then, photon echoes have been used extensively to study electronic excited state dynamics in many condensed matter systems. Recently, vibrational echoes have been used to examined vibrational dynamics in liquids and glasses.[1,16] For experiments on vibrations, a source of picosecond IR pulses is tuned to the vibrational transition of interest. The vibrational echo experiment involves a two-pulse excitation sequence. The first pulse places each molecule's vibration into a superposition state, which is a coherent mixture of the $v = 0$ and $v = 1$ vibrational levels. Immediately after the first pulse, the vibrational dipoles oscillate in phase. Because there is an inhomogeneous distribution of vibrational transition frequencies, the individual dipoles oscillate with some distribution of frequencies. Thus, the initial phase relationship is very rapidly lost. This is the vibrational free induction decay. After a time, τ, a second pulse, traveling along a path making an angle θ with that of the first pulse, passes through the sample. This second pulse changes the phase factors of each vibrational superposition state in a manner that initiates a rephasing process. At time τ after the second pulse, the sample emits a third coherent pulse of light. The emitted pulse propagates along a path that makes an angle 2θ with the path of the first pulse. The third pulse is the vibrational echo. It is generated when the ensemble of microscopic dipoles is rephased at time 2τ.

The rephasing at 2τ has removed the effects of the inhomogeneous broadening. However, fluctuations due to coupling of the vibrational mode to the environment cause the oscillation frequencies to fluctuate. Thus, at 2τ there is not perfect rephasing. As τ is increased, the fluctuations produce increasingly large accumulated phase errors among the microscopic dipoles, and the intensity of the echo is reduced. A measurement of the echo intensity vs τ, the delay time between the pulses, is called an echo decay curve. The Fourier transform of the echo decay is directly related to the homogeneous line shape.[19] An exponential vibrational echo decay corresponds to a Lorentzian line shape with a width, Γ, given by

$$\Gamma = \frac{1}{\pi T_2} = \frac{1}{\pi T_2^*} + \frac{1}{2\pi T_1} \tag{1}$$

T_2 is the homogeneous dephasing time determined from the echo decay constant. T_1 is the vibrational lifetime determined from pump−probe experiments. Measurements of T_2 and T_1 permit the determination of T_2*, the pure dephasing contribution to the line width. In liquids, there is an additional contribution from orientational relaxation.[16] However, in the experiments presented below, orientational relaxation does not occur on the time scale of the experiments because of the large size of the protein and the high viscosity of the solvent. This was confirmed with polarization selective pump−probe experiments. T_2 is determined from the vibrational echo decay signal, $S(\tau)$, given by

$$S(\tau) = S_o e^{-4\tau/T_2} \tag{2}$$

The vibrational echo and pump−probe experiments were performed at the Stanford Free Electron Laser (FEL) Center. The electron beam from a superconducting linear accelerator is directed into a magnetic wiggler at the center of an optical resonator. The electron beam interacts with the intracavity radiation, emitting photons coherently at an energy corresponding to the Doppler-shifted spatial frequency of the wiggler. The

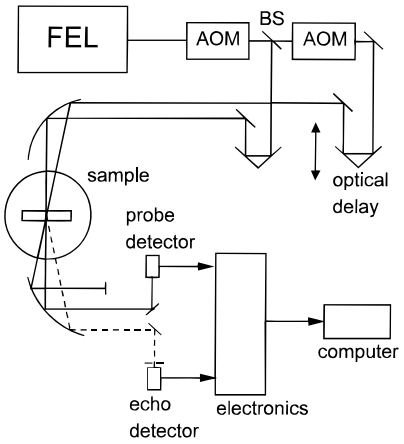

Figure 1. Schematic of the apparatus used to perform the echo and pump−probe experiments. AOM denotes Ge acousto-optic modulators used as pulse selectors. BS denotes beam splitter. The path of the echo signal emitted by the sample is indicated by the dashed line. The differences between the two setups involve the choice of beam splitter (50% *R* for echo, 10% *R* for pump−probe), in the optical pulse sequence selected by the AOMs, and in the detectors.

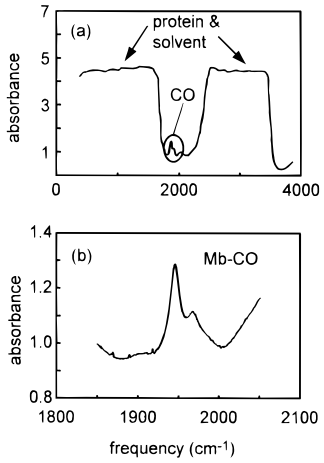

Figure 2. (a) Mid-IR spectrum of Mb−CO in glycerol/water. The circled region indicates the location of the CO vibrational fundamental transition on top of a broad background from protein and solvent. (b) Blow up of the CO stretching transition. The experiments are conducted on the large peak (A_1). The small peak to higher frequency is the A_0 band associated with another Mb−CO conformer.

FEL pulse train consists of a macropulse of about 3 ms length repeating at 10−20 Hz, within which is contained a series of micropulses repeating at 11.8 MHz. Each micropulse has an energy of ∼1 μJ. These micropulses are transform-limited Gaussians. In the experiments, the pulse duration was ∼1.7 ps. The FEL frequency, tuned to 1945 cm^{-1} for the experiments, is actively stabilized to within 2×10^{-2}% of the center frequency. Both the autocorrelation and the spectrum are monitored continuously. Although the experiments were performed with an FEL, a source based on conventional lasers having similar characteristics may also be used.

A schematic describing the experimental apparatus used for the photon echo and pump−probe experiments is shown in Figure 1. In order to reduce the heating of the sample while retaining high peak power, single micropulses are selected from the macropulse at a reduced repetition rate of 60 kHz, using a germanium acousto-optic modulator (AOM). Each micropulse is split into two roughly equal parts to become the two input pulses in the vibrational echo sequence. One beam is sent through a motorized optical delay line after passing through a second AOM that chops it at 30 kHz. The chopping is used to do background subtraction. The two beams are subsequently focused to 100 μm diameter spots in the sample using off-axis paraboloidal mirrors. The energies of the two pulses at the sample are ∼250 and ∼150 nJ. For noncollinear input beams, phase-matching conditions cause the echo signal to emerge from the sample in a unique direction. A liquid nitrogen-cooled InSb detector is used to detect the echo signal. The entire apparatus is contained in a nitrogen purge box to remove the effects of atmospheric water absorption, thus increasing the total pulse energy at the sample as well as preventing any temporal pulse distortion effects.

The apparatus used for the pump−probe vibrational lifetime measurements is nearly identical to that used for the vibrational echo. Unlike the zero-background photon echo experiment, the pump−probe experiment requires accurate measurements of small changes in the probe amplitude. For this reason, the first AOM is used to pick two adjacent micropulses, instead of just one. These two pulses are highly correlated in amplitude, temporal width, and frequency due to the relatively high *Q*(30) of the FEL cavity. Ten percent of this beam is split off to become the probe beam. The remainder of the beam travels through the delay line and the second AOM, where the second of the two pulses is selected to become the pump pulse. These two beams are crossed in the sample. A fast, liquid nitrogen-cooled MCT detector is used to detect the individual micropulses of the probe beam. The amplitude of the first of the two probe pulses, which arrives prior to the pump pulse, is used as a reference for the second pulse. The signals from the two pulses are subtracted, and the results are recorded as a function of delay time.

The samples used for the experiments were wild type horse heart myoglobin−CO dissolved in a buffered pH = 7 glycerol/water (95%/5% w/w). The protein concentration of these samples is typical of that used in infrared experiments,[8] but the glycerol concentration is greater than the 75%/25% solutions typically used. The greater glycerol concentration improved the optical quality of the solvent glass at low temperatures, which is desirable because light from the excitation pulses scattered by the solvent glass hinders detection of the echo pulse. The samples were prepared by slowly adding lyophilized myoglobin (Sigma) to 1 mL of pure glycerol with continuous stirring until the concentration of the solution was 15 mM. The frothy solution was then allowed to settle for a few hours. The solution was saturated with CO by bubbling gas through it. Then 50 μL of a solution of sodium dithionite in pH = 7 phosphate buffer, also saturated with CO, was added to reduce the protein to allow it to bind CO. The sample was placed inside a cell with CaF_2 windows, a path length of 125 μm, and a Mb−CO concentration of 15 mM. The sample cell was placed on the cold finger of a Janis helium flow cryostat. Temperature stability was better than ±0.5 K.

Photon echo and pump−probe measurements were made approximately every 20 K from 60 to 300 K. Careful studies of the power dependence of pump−probe lifetime measurements and vibrational echo dephasing measurements were made; in both experiments, the measured decay times were constant for all input intensities. The FEL micropulse with duration 1.7 ps has a corresponding spectral width of 8.6 cm^{-1}. Polarization selective pump−probe experiments demonstrated no dependence of the decay on the probe polarization. Therefore, orientation relaxation is unimportant on the time scale of the measurements.

III. Results and Discussion

Figure 2 displays an IR spectrum of Mb−CO in the vicinity of the CO vibrational absorption, taken at ambient temperature,

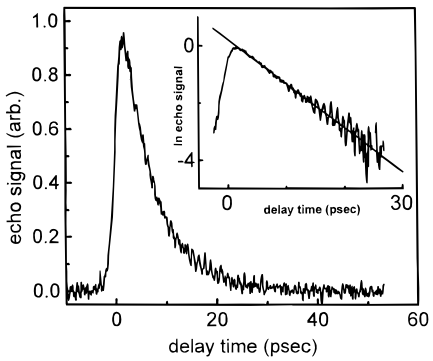

Figure 3. Vibrational echo data on Mb−CO in glycerol/water at 80 K. Inset: semilog plot (base e) shows the echo decay is exponential over a wide dynamic range. An exponential echo decay means that the homogeneous line shape is Lorentzian. At 80 K, the vibrational echo data gives a value for the dephasing time constant of $T^2 = 26.2$ ps. Therefore the homogeneous line width is 12.1 GHz (0.4 cm^{-1}). This is a factor of ∼30 narrower than the inhomogeneously broadened absorption spectrum line width.

with 2 cm^{-1} resolution. The upper panel shows a broad range of wavelengths. The enormous number of vibrational states associated with the protein and the solvent produce a significant background with an absorbance of ∼1. The Mb−CO absorption appears as a smaller feature against this background. The lower panel shows an expanded view of the Mb−CO spectrum. The CO absorption is readily seen above the broad background. It has been shown this absorption spectrum can be decomposed into four subbands.[8b] The large peak in the lower panel (∼1945 cm^{-1}) corresponds to the subband conventionally labeled A_1. The smaller peak (∼1970 cm^{-1}) corresponds to the subband conventionally labeled A_0. The intensity at ambient temperature of the A_0 subband, relative to the A_1 subband, tends to increase as the viscosity of the solvent increases,[8b] and in this 95% glycerol solvent, the A_0 transition in this spectrum is more prominent than in the more usual 75% glycerol solutions. In previous vibrational echo experiments, a system was investigated with an essentially background free spectrum.[1] However, as shown below, it is possible to obtain high-quality vibrational echo data even from a system with a congested spectrum like Mb−CO. This is because the nonlinear nature of the method eliminates the background, which arises from a large number of weak transitions.

Figure 3 shows an echo decay taken at 80 K. The main figure is a linear plot. It can be seen that the signal-to-noise ratio is very good in spite of the large amplitude of the background in the spectrum. The inset displays a semilog plot of the data. The data fall on a straight line over 4 factors of e. Therefore, the data decay exponentially, demonstrating that the homogeneous line shape is Lorentzian. The echo decays observed at all temperatures are exponential. The T_2 obtained from the 80 K data is 26.2 ps, yielding a homogeneous line width of 0.4 cm^{-1}. The width of the absorption spectrum is ∼12 cm^{-1}. Therefore, the line is massively inhomogeneously broadened; the two widths differ by a factor of ∼30.

The temperature dependence of the vibrational echo decays as well as the pump−probe lifetime measurements were obtained from 60 to 300 K. Each decay curve was fit to an exponential using a Levenberg−Marquardt fitting routine.[20] For the high-temperature echo decays, the decay times are approaching the pulse width. Therefore, the data were fit to the convolution of a Gaussian and an exponential. Care was taken in each case to verify the stability of the fit, and for most temperatures, the decay constant could be determined within ±3% for the echo data and ±5% for the pump−probe data.

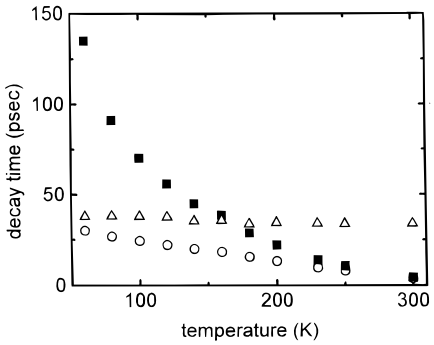

Figure 4. Temperature-dependent data. The circles are the measured values of T_2 obtained from the vibrational echo decays using eq 2. The triangles are $2T_1$. T_1 is the decay constant measured in the pump−probe vibrational lifetime experiments. From eq 1, the relevant quantity is $2T_1$. The squares are T_2*, the pure dephasing time, obtained from T_2 and $2T_1$ using eq 1.

Figure 4 shows temperature-dependent data. There are three sets of points in the figure. The circles are the measured values of T_2 obtained from the vibrational echo decays using eq 2. The triangles are $2T_1$. T_1 is the decay constant measured in the pump−probe vibrational lifetime experiment. From eq 1, it is seen that the relevant quantity is twice the lifetime, which is $2T_1$. The squares are T_2*, the pure dephasing time, obtained from T_2 and $2T_1$ using eq 1. T_1 has a very mild-temperature dependence. T_2 has a steeper temperature dependence, changing by about an order of magnitude between 60 and 300 K. The pure dephasing, T_2*, which arises from vibrational energy level fluctuations, has a very steep temperature dependence. At the lowest temperatures, the lifetime is the major contributor to the homogeneous dephasing (inverse of the line width). By room temperature, pure dephasing completely dominates the homogeneous dephasing. At all temperatures, the line is inhomogeneously broadened. At room temperature, the homogeneous line width is 2.7 cm^{-1} while the absorption spectrum width is ∼13 cm^{-1}, i.e., the absorption spectrum is ∼5 times wider than the homogeneous line width. (The absorption line width was obtained from the data in Figure 2 by taking the half-width at half-height on the red side of the line and doubling it.) The observation of inhomogeneous broadening at room temperature is important. It allows us to conclude that, on the echo time scale, the protein exists in many different distinguishable conformational substates that induce different transition frequencies of the carbonyl stretch.

The photon echo experiment is nonlinear. The signal depends on the cube of the intensity and the square of the concentration. Because of the strong dependence on intensity and concentration, when the FEL is tuned to the peak of the A_1 line, there is no contribution from the large A_0 shoulder or the small A_2 and A_3 peaks.[8b] If the FEL were tuned to the peak of the A_0 line, the signal would be down by a factor of ∼5. Because the experiments are conducted in the low-power limit, only the portion of the pulse spectrum that is resonant with a vibration can generate signal. The half-width of the pulse spectrum is 4.3 cm^{-1} and the A_0 line is shifted from the A_1 line by 25 cm^{-1}. Therefore, the intensity is so far down that no signal is generated from A_1. The FEL was tuned ±4 cm^{-1} around the peak of A_1. This change will still result in a negligible contribution from the other peaks. The vibrational echo decays and the pump−probe decays were unchanged by the shifts in wavelength, demonstrating that the dynamics are independent of the position in the inhomogeneous line over this range of wavelengths.

Figure 5 displays the pure dephasing rate, $1/T_2$*, on a log plot. It is clear from this plot that the temperature dependence

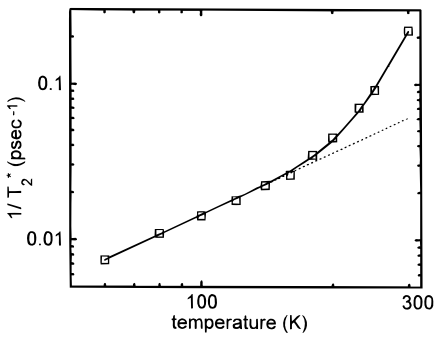

Figure 5. Plot of the natural log of $1/T_2$* vs the natural log of temperature. The solid line in the figure is a fit to the sum of a power law and an exponentially activated process, eq 3. The arrow indicates the position of the glass transition at ~185 K. Below this temperature, the data follow a power law, $T^{1.3}$ dependence, which appears linear on the log−log plot. Above ~185 K, an exponentially activated process describes the data with $\Delta E \approx 1000$ cm^{-1}.

of the pure dephasing rate is much milder at low temperatures, with a break in the temperature dependence at ~185 K, which is approximately the glass transition temperature of the glycerol/water solvent. The low-temperature data fall precisely on a straight line, indicating that the temperature dependence is described by a power law, T^{α}. The exponent of the power law can be obtained directly from the slope of the linear portion of the data, yielding $\alpha = 1.3 \pm 0.1$. A variety of functional forms were tried in the data analysis. The line through the data is a fit to the functional form of a power law plus an exponentially activated process,

$$\frac{1}{T_2^*} = aT^{\alpha} + be^{-\Delta E/kT} \qquad (3)$$

Of the many functional forms that were tried, eq 3 is the only one that provides good agreement with the data. There are two ways to obtain a fit, and they yield distinctly different activation energies but the same power law exponent. One is to assume that both terms in eq 3 are active at all temperatures, while the other assumes a change in mechanism at the solvent's glass transition. If eq 3 is used as written, as the sum of the two functions, $\Delta E = 1250$ cm^{-1}. The activated process makes little contribution at the lower temperatures. However, the power law contributes 25% at room temperature. In the second approach, at low temperature, the dephasing is given only by the power law. This does not change the value of α. At the glass transition, the dephasing becomes exponentially activated. Therefore, there is no contribution from the power law at high temperature. Using this approach, the activated process fits the data with $\Delta E = 800$ cm^{-1}. It needs to be emphasized that, while eq 3 fits the data extremely well, it cannot be proven to be unique.

The data raise several important issues: 1. Why is there a change in the form of the temperature dependence near the solvent glass transition temperature? 2. What are possible explanations for the power law temperature dependence and the exponentially activated temperature dependence? 3. What is the mechanism that couples the protein fluctuations to the CO stretching frequency, causing the pure dephasing?

In the following discussion, some initial ideas and relevant information will be presented. It is not possible to provide definitive answers to the three questions that are proposed, but it is possible to indicate directions for constructive thought. After the discussion of the three questions, some future lines of research that should be fruitful in narrowing the possibilities will be described.

1. Change in the Form of the Temperature Dependence. The helical chains that make up Mb can undergo both large-amplitude and small-amplitude motions under biological conditions.[21] However, at low temperatures, below the solvent glass transition temperature, the glassy solvent provides a rigid boundary condition for the protein. This rigid boundary condition will suppress conformational changes that would change the shape of the protein surface. Molecular dynamics simulations have demonstrated a protein's ability to sample thousands of minor conformational changes on fast time scales.[9] These are classical, room temperature calculations. As discussed below, the low-temperature dynamics may involve tunneling. The simulations, nonetheless, demonstrate the existence of many conformations that involve only small structural changes. Once the temperature is raised above the glass transition temperature, the liquid solvent provides a much softer boundary condition. The softer boundary will facilitate more significant conformational changes that need not preserve the surface shape of the protein. It will lower barriers that are insurmountable in the rigid, glassy solvent. Recent experiments using other solvents, which will be presented subsequently,[22] show that the change from a power law to an exponentially activated process follows the solvent glass transition temperature.

Evidence exists to support the supposition that Mb undergoes a transition, called the "slaved glass transition", near the glass transition temperature of the solvent.[10,23] Calorimetric measurements of Mb in glycerol/water, ethylene-glycol/water, and PVA indicate that the temperature at which this transition occurs, T_{sg}, is generally a few degrees warmer than the glass transition of the solvent itself. Studies of CO to Mb rebinding kinetics, infrared line shape, and small molecule diffusion all imply a sharp change in dynamics occurring around T_{sg}. The dynamics are characterized below T_{sg} by slow, markedly nonexponential time dependences, similar to effects seen in glasses, and, above T_{sg}, by much faster kinetics. These experiments imply a change in the nature of the dynamics at T_{sg}. It should be noted that experiments, such as rebinding kinetics, operate on a time scale of tens of microseconds to thousands of seconds, while the echo measurements are examining dynamics on the 10 ps time scale. The pure dephasing data does not show a sharp change near the slaved glass transition, but, rather, a change in the functional form of the temperature dependence.

2. The Temperature Dependence of the Pure Dephasing. In the lower temperature range (from 60 to ~185 K), the pure dephasing line width has a temperature dependence of $T^{1.3}$. This is reminiscent of the temperature dependence that has been observed for the pure dephasing of electronic transitions of molecules in low-temperature glasses using photon echo experiments.[11] In low-temperature (from 0.1 to 10 K) glasses such as ethanol, glycerol, and PMMA, the pure dephasing line widths of dye molecules display temperature dependences of T^{α}, where the most common value for α is 1.3, but α ranges from 1.2 to 1.5 for various glasses.[11] The similarity is so striking that it is worth discussing the nature of the model that gives rise to this temperature dependence. Comparing proteins to glasses has a significant history. The two basic hallmarks of a glassy system, the long-range disorder and the multiple energy minima, are found in protein systems as well. There exists experimental evidence that is used to support the comparisons. Measurements of the nonexponential time dependence of the rebinding kinetics of O_2 and CO at low temperature were interpreted, early on, in terms of glassy behavior in proteins.[24] Later, measurements found that the low-temperature (1 K) heat capacities of proteins mimic the near linear behavior of glasses.[25] More recent measurements of the pressure and temperature dependence of

the mid-IR absorption bands of Mb−CO have shown nonexponential time dependence and non-Arrhenius temperature dependence of the pressure relaxation as a function of temperature.[26] These observations have all been interpreted as evidence for a similarity between proteins and glasses.

Glasses are systems which, unlike crystals, possess no long-range translational or rotational order and are not in a state of thermodynamic equilibrium.[27] Glass properties are determined by a combination of the dynamics of quasi-phonons (the disordered equivalent of phonons in a crystal) and by the additional dynamics introduced by the evolution of local glass conformations. Extensive experimental studies have clarified the differences between glasses and crystals.[12] The heat capacity in a crystal obeys the Debye T^3 dependence at low temperature; in a glass, there is an additional term, approximately linear in temperature below a few degrees K. In a crystal, the thermal conductivity varies as T^3, while in a glass, the temperature dependence at low temperature is T^2. Several theoretical models have been developed to explain the various observations. However, the two-level system (TLS) model has enjoyed the most success.[13]

The possible local conformations of a glass are associated with an extremely complex, multidimensional potential surface. The TLS model simplifies the description of dynamics on this potential surface. The TLS model postulates that some atoms or molecules (or groups of atoms or molecules) can reside in either of only two minima of the local potential surface. Each side of the double-well potential represents a distinct local structural configuration of the glass. The bulk glass material contains an ensemble of these two-level systems, having a broad distribution of energy differences and tunneling parameters. At low temperatures, transitions occur via tunneling through the potential barriers or, at sufficiently high temperatures, by activation over these barriers. Thus, the complex potential surface is modeled as a collection of double-well potentials.

Using this simple physical picture, the TLS model simulates the rugged, multidimensional energy potential surfaces that exist in glasses. The agreement of the predictions of the theory with experimental data is striking; the model reproduces the temperature dependence of the heat capacity and thermal conductivity.

Optical dephasing of chromophores in low-temperature glasses is caused by the coupling of the optical centers to the TLS dynamics. When the TLS undergoes transitions via tunneling between the two wells, the associated changes in local structures cause the transition energy of a chromophore to fluctuate. Because there is a wide range of tunneling parameters, λ, and energy differences, E, between the sides of the two wells, there is a broad range of rates of transitions between the wells. This broad distribution of tunneling rates produces a broad range of rates of chromophore energy fluctuations. The temperature dependence of the electronic excited state pure dephasing line width measured in photon echo experiments on molecules in glasses at low temperatures can be calculated using the TLS uncorrelated sudden jump model.[28] More complex models give similar results.[29] It is found that the temperature dependence is

$$\frac{1}{T_2^*} = aT^{\alpha} \tag{4}$$

where α is determined by $P(E)$, the probability distribution for the TLS energy difference E. If $P(E)$ equals a constant, i.e., there is equal probability of all TLS splittings and the distribution of tunneling parameters is also flat, then $\alpha = 1$. In general, for

$$P(E) \propto E^{\mu} \tag{5a}$$

$$\alpha = 1 + \mu \tag{5b}$$

Therefore, the typical temperature dependence observed for electronic dephasing in the temperature range below 5 K indicates an almost flat distribution of TLS energy splittings and an essentially flat distribution of tunneling parameters. These distributions are consistent with the observed heat capacities, which are described by the same model and parameters.

Prior to discussing the vibrational dephasing of Mb−CO caused by protein fluctuations using the PTLS model, which is analogous to the glassy TLS model, it is important to present the strong evidence that Mb−CO dephasing is not caused by the solvent.

For the solvent to cause dephasing, it must couple to the transition frequency of the CO. When molecules go from the gas phase to a condensed matter environment, there is a shift of the transition frequency. This is true of both electronic transitions and vibrational transitions. This shift is referred to as the solvent shift. Molecular interactions with the condensed matter environment are responsible for line broadening as well as the solvent shift. These two are closely related. The line broadening can be static, giving rise to an inhomogeneous line, or dynamic, giving rise to a homogeneous line. In either case, variations in the solvent shift cause line broadening.

In Mb−CO, the nature of the solvent itself has little effect on the CO vibrational transition frequency. The Mb−CO transition frequency is virtually identical whether the solvent is water (1944 cm^{-1}),[8b] 75% glycerol/water (1945 cm^{-1}),[8b] poly(vinyl alcohol) (1946 cm^{-1}),[8b] trehalose (1945 cm^{-1}),[30a] or a Mb crystal (1946 cm^{-1}).[30b] These values are all within the error of the determination of the peak center. The solvent shift is unaffected by the medium surrounding the protein even when the change is from a liquid solvent to a protein crystal. In contrast, the frequency difference between the Mb−CO A_o and A_1 lines is 25 cm^{-1}.[8b] This difference is caused by a change in the distal histidine. Changes in the protein structure have a major influence on the transition frequency while changes in the solvent have a negligible influence. This leads to the reasonable conclusion that fluctuations of the protein structure will cause homogeneous dephasing while fluctuations of the solvent structure will not. Of course, the solvent provides a heat bath and a boundary condition that are intimately involved in the protein fluctuations and the dephasing, but the argument made above strongly supports the idea that the dephasing does not arise from direct coupling of the solvent dynamics to the CO transition frequency.

The TLS properties of glasses are only manifested at very low temperatures. In the 60−185 K temperature range under discussion, TLS dynamics are overwhelmed by the quasi-phonon dynamics of a glass.[11,31] The barrier heights in glasses are too low for the dynamics to still involve tunneling processes at the elevated temperatures of these experiments,[31] and it is tunneling that gives rise to the power law temperature dependence with $\alpha \approx 1$.

The experiments that are most directly comparable to those presented in this paper are vibrational echo measurements conducted on the asymmetric CO stretching mode (1980 cm^{-1}) of $W(CO)_6$ in three liquid/glass solvents, 2-methylpentane, 2-tetrahydrofuran, and dibutyl phthalate.[16] While $W(CO)_6$ is not the same as CO bound to Fe−heme, the experiments provide vibrational dephasing information for a CO stretching mode of a metal carbonyl in glassy solvents in the same temperature

range as the Mb−CO experiments. Although the three glasses are quite different from each other, $W(CO)_6$ vibrational dephasing has an identical T^2 dependence in all three. The T^2 temperature dependence is consistent with a dephasing mechanism that occurs in glasses at high temperatures. It arises in the high-temperature limit from activation over potential barriers. It is a two-phonon scattering process in which one phonon is annihilated to take the system above a barrier and a second phonon is created when the system relaxes into the other side. In inorganic glasses, optical dephasing of electronic states at elevated temperatures is also observed to have a T^2 temperature dependence.[32] This is the hallmark of activation over barriers at high temperatures, rather than tunneling.

$W(CO)_6$ vibrational dephasing was also studied above the glass transition temperature.[16] There is a very sharp increase in the slope of the temperature dependence at the glass transition temperature. However, unlike the results presented here, the temperature dependence for $W(CO)_6$ vibrational dephasing in 2-methylpentane liquid is not exponentially activated, but rather obeys a Vogel−Tammann−Fulcher (VTF) equation.[33] The VTF equation has the form

$$f(T) = \beta e^{-D/(T-T^*)} \tag{6}$$

where $f(T)$ is a temperature-dependent quantity, in this case the pure dephasing time, and T^* is a critical temperature. The functional form is much steeper than an activated process since it diverges at the glass transition temperature. It was found that a VTF form cannot fit the data in Figure 4, regardless of the choice of parameters. It is far too steep.

Thus, vibrational dephasing of a metal carbonyl in glass forming liquids has a temperature dependence that is much steeper both in the glass and in the liquid than the Mb−CO dephasing over the same temperature range. The observed differences help confirm that the vibrational pure dephasing of Mb−CO is caused by protein fluctuations rather than direct coupling to the solvent dynamics.

The $T^{1.3}$ pure dephasing temperature dependence of Mb−CO in the lower temperature portion of Figure 5 is consistent with a tunneling TLS model of the protein. To apply a protein-tunneling TLS model requires describing the ensemble of protein molecules in the following manner. A protein in the ensemble is a nonequilibrium system with many possible conformations. Conformational changes can be viewed as occurring via motion on a multidimensional potential surface. Such a surface has frequently been referred to as the energy landscape. Three types of dynamics can occur. Motions that do not move the system from one point to another on the surface are vibrations. These can be high-frequency vibrations of small groups such as a C−H stretch or low-frequency motions that involve larger sections of the protein backbone. These motions are fluctuations about a local minimum on the surface. They do not change the protein conformation. Other motions move the system from one point on the energy landscape to another. These are conformational changes and can occur via tunneling through a potential barrier from one minimum to another, or they can occur by activation over a barrier. In either case, the system will pass from one local minimum to another.

If the system is in one local minimum of the multidimensional potential surface, at relatively low temperature the vast majority of the barriers to movement to other minima may be so high that both tunneling through or activation over the barriers is impossible. However, from this point on the landscape there may be one other conformation that can be reached by tunneling. The PTLS model represents this complex potential surface as a collection of double well potentials. There is a broad distribution of differences in energy E between the two sides of the double wells. Each side of a double well represents a conformation on the energy landscape. There is also a distribution of barrier heights V and tunneling parameters λ. (For a barrier modeled as an inverted parabola, the probability of tunneling goes as $e^{-\lambda}$, with $\lambda = d(2mV/h^2)^{1/2}$; d is the distance through the barrier, and m is the mass.) The tunneling PTLS model describes the fluctuations in protein conformations as tunneling between the two sides of the PTLS. There are many PTLSs, and each transition of a particular PTLS represents a specific conformational change of the protein.

Although activation does not occur over barriers, the thermal energy of the protein still plays a role because the two sides of the PTLS, in general, have different energies. To move from the low-energy side to the high-energy side requires the absorption of a phonon from the protein. To move from the high-energy side to the low-energy side requires emission of a phonon. In the protein, the continuum of very low frequency vibrations[34] serves the role of the phonon continuum in a glass.

Since there are many PTLSs in each protein, there are many conformational fluctuations occurring with a distribution of rates, $P(R)$, determined by the distributions of E and λ, i.e., $P(E)$ and $P(\lambda)$. As the temperature is raised, the occupation numbers of the proteins' low-frequency vibrational modes increase. The increase causes faster transitions between the sides of the active PTLS and also allows PTLSs that were inactive because E was too large to become active. Fluctuations in the protein structure, which correspond to transitions between sides of the PTLS, are coupled to the vibrational frequency of the CO. These fluctuations in structure cause fluctuations in the vibrational frequency, giving rise to pure dephasing.

In a protein, there will be a large number of PTLSs each undergoing jumps between two states. If these jumps are uncorrelated, i.e., a transition in one PTLS does not influence the probability of a transition in another PTLS, then theoretical work developed to describe dynamics in low-temperature glasses can be applied to the vibrational dephasing problem in Mb−CO.[28] In the context of the uncorrelated sudden jump model, from eqs 4 and 5, the observed $T^{1.3}$ temperature dependence implies that $P(E) \propto E^{0.3}$.

This is a very flat distribution of energies. The PTLS model of the Mb protein indicates that the protein has an energy landscape on which conformational changes occur via tunneling, and the distribution of energy differences between conformations is very broad and almost flat. The tunneling rate must be sufficiently fast to cause vibrational pure dephasing on a 10 ps time scale. The essentially flat energy landscape does not have to extend over all energies to be consistent with the data. PTLSs with energies splittings greater than ~2 kT contribute little to the dephasing. Thus, there can be a deviation from $E^{0.3}$ or even a cut off at high energy which will not influence the observed temperature dependence. Furthermore, there can be a distribution of very low energy barriers that will not come into play. Electronic dephasing experiments conducted on heme proteins at very low temperature (2 K) have been interpreted in terms of very low barriers to structural changes.[2] In the current experiments, such a set of barriers will be so low in energy that they do not impose constraints on the dynamical motions in the 100 K range. The set of low barriers can be viewed as slight roughness of the bottoms of the potential wells that are involved in the dynamics at higher temperatures. The low-temperature and high-temperature results suggest there is a set of very low barriers involved in the very low temperature dynamics and a set of relatively high barriers that is involved in the higher temperature dynamics and a gap in between. If

the distribution of barrier heights were continuous, then, at the elevated temperatures of these experiments, a significant amount of the conformational dynamics would involve activation over the intermediate barriers. Such a situation is inconsistent with the PTLS model that gives rise to the observed $T^{1.3}$ temperature dependence.

The PTLS model of the Mb protein is consistent with molecular dynamics simulations which show many conformations with transitions occurring on a picosecond time scale.[9] However, the simulations are classical and at high temperature. They do not address the question of tunneling. Nonetheless, they do indicate a complex energy landscape with many local minima, a prerequisite for the PTLS model.

Within the context of the uncorrelated sudden jump model of vibrational dephasing, two other restrictions are placed on the system to be consistent with the experimental data.[28] As shown in Figure 3, the vibrational echo data decay exponentially. To obtain the observed temperature dependence and an exponential decay requires that the coupling of the PTLS to the CO vibrational transition frequency falls off as $1/r^3$, where r is the distance of a PTLS to the CO or probably the heme (see below). Also the distribution of PTLS fluctuation rates, $P(R) \propto 1/R$, where R is the rate of fluctuation (jumps).[28] Other theoretical descriptions of TLS dynamics and optical dephasing in low-temperature glasses place similar restrictions on the coupling and rate distribution.[29] Dipolar coupling and a $\sim 1/R$ fluctuation rate distribution are believed to occur in glasses at low temperatures. A theoretical investigation is currently in progress to determine if a less restrictive, non-PTLS model of protein fluctuations can account for the observed power law temperature dependence.[35] This model still involves an energy landscape with a broad distribution of barriers and transitions among a limited set of protein conformations, but it does not require a specific coupling mechanism or a $1/R$ distribution of fluctuation rates.

Above the solvent glass transition temperature, the vibrational pure dephasing line width appears to be exponentially activated. As discussed above, the change in the temperature dependence may be attributed to the softening of the boundary condition placed on protein motions by the solvent. The rigid glass boundary may permit only conformational changes that preserve the surface shape of the protein. When the solvent is a liquid, protein conformational changes that involve changes in the surface shape become possible. Barriers to conformational change that were insurmountable with the rigid glassy boundary condition become lower when the solvent is a liquid. The result is a distinct change in the energy landscape. Conformational changes that were impossible below the solvent glass transition can occur via activation over barriers. The activated conformational changes can replace the $T^{1.3}$ process as the dominant mechanism for protein fluctuations. The activated process does not arise from excitation of a particular vibrational mode of the protein since the break in the functional form of the temperature dependence tracks the glass transition temperature when the solvent is changed.[22]

As discussed above in connection with the fit of the data to eq 3, it is not possible to determine if there is a change from the $T^{1.3}$ mechanism to activated barrier crossing or if the power law portion persists to high temperatures. If the activated pathways involve conformational changes that cannot occur by tunneling, then the number of tunneling events per unit time will decrease and possibly become unimportant. Therefore, there is a range of possible activation energies that fall between $\Delta E = 1250$ cm^{-1} (power law continues to high temperature) and $\Delta E = 800$ cm^{-1} (power law unimportant at high temperatures). The net result is that $\Delta E \approx 1000$ cm^{-1}, but this number is uncertain to several hundred cm^{-1}. Since the activated temperature dependence is observed over a relatively narrow range of temperature, the single activation energy could actually represent a distribution of ΔE values. It is important to emphasize that only those structural changes that influence the CO vibrational energy are manifest in the vibrational echo pure dephasing temperature dependence.

3. Mechanism of Coupling Protein Fluctuations to the CO Vibrational Frequency. Vibrational pure dephasing is caused by fluctuations in the vibrational transition energy.[16] For protein conformational changes to cause pure dephasing there must be a mechanism that couples the protein dynamics to the CO vibrational energy.

In the literature of the vibrational spectroscopy of CO bound to metalloporphyrins, model hemes, myoglobin, and mutant myoglobins, it is well established that static shifts in the vibrational frequency of the CO stretch are caused by changes in back-donation of electron density from the extended metal−macrocycle π system to the CO π^* antibonding molecular orbital.[36] The back-donation is referred to as back-bonding. The π system of the macrocycle is a superposition of the metal d_π and ring nitrogen and carbon p_π orbitals. Electron density is transferred to the empty CO π^* orbital. Electron density in the π^* orbital reduces the strength of the CO bond and, therefore, lowers the vibrational frequency. In model compounds, when Fe is replace by Ru, and then by Os, the vibrational frequency shifts progressively to lower energy.[37] As the metal atom becomes larger, the d orbitals are larger and more diffuse, resulting in more back-bonding. Changes in substituents on the porphyrin are also correlated with changes in back bonding and frequency shifts. In Mb and mutant Mb's, changes in particular amino acids influence back-bonding via changes in local electric fields that influence the macrocycle electron density and therefore the back-bonding.[5]

Recently, back-bonding has been shown to be intimately involved in CO vibrational lifetime dynamics in model hemes and in Mb and mutant Mb's.[37,38] The vibrational lifetimes of CO bound to 37 model compounds and 7 Mb's were found to be related to the vibrational frequency of the CO. As the frequency shifts to the red, the rate of vibrational relaxation becomes larger. The relationship between frequency and relaxation rate is essentially linear. A 3% change in vibrational frequency results in an approximately 3-fold change in the vibrational relaxation rate. As the back-bonding increases, the coupling of the CO to the heme increases, and the vibrational relaxation rate increases.

Static changes in back-bonding cause changes in the CO vibrational frequency and cause changes in the vibrational lifetime. Therefore, we propose that the basic mechanism for the Mb−CO vibrational pure dephasing involves fluctuations in the back-bonding. Fluctuations in back-bonding will cause fluctuations in the CO vibrational frequency just as static changes in back-bonding cause static shifts in the CO energy. We suggest two possible paths by which fluctuations in protein structure influence the back-bonding and, therefore, cause the vibrational pure dephasing. One we term the electric field mechanism and the other, the mechanical mechanism.

The electric field mechanism depends on the fact that the heme−CO subsystem is surrounded by the protein, which contains polar groups, e.g., the distal histidine. Fluctuations in the protein conformation will produce time varying electric fields at the heme. These time dependent fields will in turn cause modulations of the macrocycle electron density distribution. The time-dependent variations in electron density will cause fluctua-

tions in the back-bonding and, therefore, CO vibrational transition frequency fluctuations, i.e., pure dephasing.

The mechanical mechanism involves the fact that the heme−CO subsystem is coupled to the protein by only one covalent bond. The proximal histidine, which is the ligand bound to the metal on the opposite side of the heme from the CO, makes the only covalent bond to the protein. From CO photodissociation experiments, it is known that movement of the Fe out of the plane of the macrocycle is mechanically coupled to the protein through the proximal histidine.[7] In the mechanical pure dephasing mechanism, as the protein undergoes conformational fluctuations, the proximal histidine, like a piston, pushes and pulls the Fe in and out of the plane of the heme ring system. The Fe motion produces modifications of the π system's electron density distribution. The electron density fluctuations will, in turn, cause the back-bonding to fluctuate and therefore induce pure dephasing.

Both of the proposed mechanisms involve protein conformational motions that modulate the heme back-bonding. Both mechanisms provide the coupling between the protein motions and the CO vibrational transition energy necessary to cause pure dephasing. At this time, it is not possible to determine which of the mechanisms is dominant. However, it should be possible to address the nature of the mechanism in the future by performing temperature-dependent vibrational echo experiments on a mutant Mb in which the proximal histidine is removed and replaced by a ligand not covalently bonded to the protein and on a mutant Mb in which the distal histidine is replaced with valine. Changes in the pure dephasing of the mutants will provide insights into the coupling mechanism.

IV. Concluding Remarks

In this paper, we have described the first application of vibrational echoes to the study of protein dynamics. The vibrational echo experiment makes it possible to remove the inhomogeneous broadening from a vibrational spectrum and obtain the dynamical information contained in the homogeneous spectrum. Using the Stanford FEL as a source, we have performed vibrational echo and lifetime relaxation measurements on CO bound to the active site of myoglobin. Combining the results of the two types of experiments, we have obtained the pure dephasing time, T_2^*, at a series of temperatures from 60 K to room temperature. T_2* is a measure of the vibrational energy fluctuations induced by conformational fluctuations of the protein. It is found that the CO vibrational line is inhomogeneously broadened at all temperatures including room temperature. Thus, even at room temperature, the ensemble of protein molecules exists in a distribution of conformational substates that interconvert slowly compared to the 10 ps time scale of the echo experiments.

At low temperatures, the pure dephasing contribution to the homogeneous line width increases as a power law, $T^{1.3}$. Above the solvent glass transition temperature, the temperature dependence becomes exponentially activated. The change in the functional form of the temperature dependence is attributed to the softening of the boundary condition imposed on protein chain motions when the solvent (glycerol/water) becomes liquid. This view will be tested in subsequent experiments by using other solvents with different glass transitions temperatures. A protein two-level system (PTLS) model of protein dynamics, equivalent to the TLS model of glasses, was discussed. The characteristics of protein dynamics required to give rise to the observed temperature dependence are described in the context of the PTLS dynamics. This model places considerable restrictions on the nature of the protein dynamics if all observations are to be explained. A theoretical investigation is in progress to determine if a less restrictive model, which does not involve PTLS dynamics, can reproduce the observed results.

A general mechanism was proposed to explain how conformational fluctuations of the protein couple to the vibrational transition energy to cause pure dephasing. It is known that static changes in heme back-bonding to the CO antibonding π* molecular orbital result in changes in the transition energy of the CO vibration. It was proposed that protein conformational fluctuations cause fluctuations in the back-bonding and, therefore, cause pure dephasing. Two possible mechanisms through which the protein conformational fluctuations can cause modulation of the back-bonding were put forward. One is how protein induced fluctuating electric fields influence the heme, and the other is how protein induced fluctuations of the proximal histidine position causes structural perturbations of the heme. Future experiments will address these mechanisms by performing vibrational echoes on mutant Mb's.

These first vibrational echo experiments on proteins have provided a new method for examining protein dynamics at biologically relevant temperatures and have already yielded some intriguing insights into how protein dynamics are transmitted to the active site of myoglobin. The vibrational echo is the ps IR vibrational analog of the spin echo of NMR. The advent of the spin echo in 1950 ushered in a new dimension in magnetic resonance spectroscopy. The spin echo is the simplest coherent pulse sequence in magnetic resonance, yet it is the precursor to all of the important pulse sequences that are now used routinely in magnetic resonance. Without coherent pulse sequences, NMR would not be the powerful probe of structure and dynamics that it is today. As the spin echo did for NMR, the vibrational echo is expanding scope of IR vibrational spectroscopy.

Acknowledgment. This research was supported by the Medical Free Electron Laser Program, through the Office of Naval Research, Contract N00014-94-1-1024 (C.W.R., M.D.F., A.K., H.A.S.). Additional support was provided by the Office of Naval Research, Biology Division, Contract N00014-95-1-0259, the National Science Foundation, Division of Materials Research Grant DMR94-04806 (D.D.D., J.R.H.), and the National Science Foundation, Division of Materials Research, Grant DMR93-22504 (K.R., M.D.F.). We thank Professor Steven G. Boxer, Stanford University, Professor Robin Hochstrasser, University of Pennsylvania, and Professor Kenneth Suslick, University of Illinois at Urbana, for informative conversations pertaining to this research.

References and Notes

(1) Tokmakoff, A.; Zimdars, D.; Urdahl, R. S.; Francis, R. S.; Kwok, A. S.; Fayer, M. D. *J. Phys. Chem.* **1995**, *99*, 13310. Tokmakoff, A.; Fayer, M. D. *Acc. Chem. Res.* **1995**, *20*, 437.

(2) Leeson, D. T.; Wiersma, D. A. *Phys. Rev. Lett.* **1995**, *74*, 2138.

(3) Antonini, E. B. *Hemoglobin and Myoglobin in their Reactions with Ligands*; North Holland: Amsterdam, 1971.

(4) Kuriyan, J. W. S.; Karplus, M.; Petsko, G. A. *J. Mol. Biol*. **1986**, *192*, 133. Quillin, M. L.; Arduini, R. M.; Olson, J. S.; Phillips, G. N., Jr. *J. Mol. Biol*. **1993**, *234*, 140.

(5) Oldfield, E., Guo, K.; Augspurger, J. D.; Dykstra, C. E. *J. Am. Chem. Soc*., **1991**, *113*, 7537.

(6) DeBrunner, P. G.; Frauenfelder, H. *Annu. Rev. Phys. Chem.* **1982**, *33*, 283. Frauenfelder, H.; Parak, F.; Young, R. D. *Annu. Rev. Biophys. Biophys. Chem.* **1988**, *17*, 451.

(7) Petrich, J. W.; Martin, J. L. In *Time-Resolved Spectroscopy*; Clark, R. J. H., Hester, R. E., Eds.; Wiley: New York, 1989; p 335. Friedman, J. M.; Rousseau, D. L.; Ondrias, M. R. *Annu. Rev. Phys. Chem.* **1982**, *33*, 471

(8) (a) Alben, J. O.; Caughy, W. S. *Biochemistry* **1968**, *7*, 175. Caughey, W. S.; Shimada, H.; Choc, M. C.; Tucker, M. P. *Proc. Natl. Acad. Sci. U.S.A.* **1981**, *78*, 2903. Alben, J. O.; Beece, D.; Bowne, S. F.; Doster, W.;

Eisenstein, L.; Frauenfelder, H.; Good, D.; McDonald, J. D.; Marden, M. C.; Moh, P. P.; Reinisch, L.; Reynolds, A. H.; Shyamsunder, E.; Yue, K. T. *Proc. Natl. Acad. Sci. U.S.A.* **1982**, *79*, 3744. (b) Ansari, A.; Berendzen, J.; Braunstein, D.; Cowen, B. R.; Frauenfelder, H.; Hong, M. K.; Iben, I. E. T.; Johnson, J. B.; Ormos, P.; Sauke, T. Scholl, R.; Schulte, A.; Steinbach, P. J.; Vittitow, J.; Young, R. D. *Biophys. Chem.* **1987**, *26*, 337.

(9) Elber, R.; Karplus, M. *Science* **1987**, *235*, 318.

(10) Iben, I. E. T.; Braunstein, D.; Doster, W.; Frauenfelder, H.; Hong, M. K.; Johnson, J. B.; Luck, S.; Ormos, P.; Schulte, A.; Steinbach, P. J.; Xie, A.; Young, R. D. *Phys. Rev. Lett.* **1989**, *62*, 1916.

(11) Narasimhan, L. R.; Littau, K. A.; Pack, D. W.; Bai, Y. S.; Elschner, A.; Fayer, M. D. *Chem. Rev.* **1990**, *90*, 439 and references contained therein.

(12) Phillips, W. A., Ed.; *Amorphous Solids. Low Temperature Properties, Topics in Current Physics*; Springer, Berlin, 1981; Vol. 24. Stevels, J. M. The Structural and Physical Properties of Glass. In *Encyclopedia of Physics*, Flügge, S., Ed.; (Thermodynamics of Liquids and Solids). Springer-Verlag: Berlin, 1962; Vol. 13.

(13) Anderson, P. W.; Halperin, B. I.; Varma, C. M. *Philos. Mag.* **1972**, *25*, 1. Phillips, W. A. *J. Low Temp. Phys.* **1972**, *7*, 351.

(14) Gordon, R. G. *J. Chem. Phys.* **1965**, *43*, 1307. Gordon, R. G. *Adv. Magn. Reson.* **1968**, *3*, 1. Berne, B. J. In *Physical Chemistry: An Advanced Treatise*; Henderson, D., Ed.; Academic Press: New York, 1971; Vol. VIIIB.

(15) Loring, R. F.; Mukamel, S. *J. Chem. Phys.* **1985**, *83*, 2116.

(16) Tokmakoff, A.; Fayer, M. D. *J. Chem. Phys.* **1995**, *102*, 2810.

(17) Hahn, E. L. *Phys. Rev.* **1950**, *80*, 580.

(18) Kurnit, N. A.; Abella, I. D.; Hartmann, S. R. *Phys. Rev. Lett.* **1964**, *13*, 567. Abella, I. D.; Kurnit, N. A.; Hartmann, S. R. *Phys. Rev.* **1966**, *141*, 391.

(19) Farrar, T. C.; Becker, D. E. *Pulse and Fourier Transform NMR* , Academic Press: New York, 1971. Skinner, J. L.; Andersen, H. C.; Fayer, M. D. *J. Chem. Phys.* **1981**, *75*, 3195.

(20) Marquardt, D. W. *J. Soc. Ind. Appl. Math.* **1963**, *2*, 431.

(21) Frauenfelder, H.; Petsko, G. A.; Tsernoglou, D. *Nature* **1979**, *280*, 558. Brooks, C. L.; Karplus, M.; Pettitt, B. M. *Advances Physical Chemistry*; Wiley: New York, 1988; Vol. LXXI. Li, H.; Elber, R.; Straub, J. E. *J. Biol. Chem.* **1993**, *268*, 17908. Elber, R; Karplus, M. *J. Am. Chem. Soc.* **1990**, *112*, 9161. Straub, J. E.; Karplus, M. *Chem. Phys.* **1991**, *158*, 221.

(22) Rella, C. W.; Kwok, A.; Rector, K.; Hill, J. R.; Schwettman, H. A.; Dlott, D. D.; Fayer, M. D. *J. Chem. Phys.* **1996**, in preparation.

(23) Frauenfelder, H.; Alberding, N. A.; Ansari, A.; Braunstein, D.; Cowen, B. R.; Hong, M. K.; Iben, I. E. T.; Johnson, J. B.; Luck, S.; Marden, M. C., Mourant, J. R.; Ormos, P.; Reinisch, L.; Scholl, R.; Schulte, A.; Shyamsunder, E.; Sorensen, L. B.; Steinbach, P. J.; Xie, A.; Young, R. D.; Yue, K. T. *J. Phys. Chem.* **1990**, *94*, 1024.

(24) Austin, R. H.; Beeson, K.; Eisenstein, L.; Frauenfelder, H.; Gunsalus, I. C.; Marshall, V. P. *Phys. Rev. Lett.* **1974**, *32*, 403.

(25) Phillips, W. A. *Rep. Prog. Phys.*, **1987**, *50*, 1657.

(26) Iben, I. E. T.; Baunstein, D.; Doster, W.; Frauenfelder, H.; Hong, M. K.; Johnson, J. B.; Luck, S.; Ormos, P.; Schulte, A.; Steinbach, P. J.; Xie, A. H.; Young, R. D. *Phys. Rev. Lett.* **1989**, *62*, 1916.

(27) Zeller, R. C.; Pohl, R. O. *Phys. Rev. B* **1971**, *4*, 2029.

(28) Berg, M.; Walsh, C. A.; Narasimhan, L. R.; Littau, Karl A.; Fayer, M. D. *J. Chem. Phys.* **1988**, *88*, 1564. Bai, Y. S.; Fayer, M. D. *Phys. Rev. B* **1989**, *39*, 11066.

(29) Silbey, R., private communication, to be published.

(30) (a) Hill, J. R.; Dlott, D. D.; Fayer, M. D., unpublished results. (b) Ivanov, D.; Sage, J. T.; Keim, M.; Powell, J. R.; Asher, S. A.; Champion, P. M. *J. Am. Chem. Soc.* **1994**, *116*, 4139.

(31) Freidrich, J.; Harrer, D. In *Optical Spectroscopy of Glasses*; Zschokke, I., Ed.; R. Reidel Publishing Company: Dordrecht, The Netherlands, 1986.

(32) Macfarlane, R. M.; Shelby, R. M. *J. Lumin.* **1987**, *36*, 179.

(33) Angell, C. A. *J. Phys. Chem. Solids* **1988**, *49*, 863. Angell, C. A. *J. Phys. Chem.* **1982**, *86*, 3845. Fredrickson, G. H. *Annu. Rev. Phys. Chem.* **1988**, *39*, 149.

(34) Go, N.; Noguti, T.; Nishikawa, T. *Proc. Natl. Acad. Sci. U.S.A.* **1983**, *80*, 3696. Roitberg, A.; Gerber, R. B.; Elber, R.; Ratner, M. A. *Science* **1995**, *268*, 1319.

(35) Rella, C. W.; Fayer, M. D., to be published.

(36) Cotton, F. A.; Wilkinson, G. *Advanced Inorganic Chemistry*; Wiley-Interscience: New York, 1988; p 57. Boldt, N. J.; Goodwill, K. E.; Bocian, D. F. *Inorg. Chem.* **1988**, *27*, 1188. Spiro, T. G. In *Iron Porphyrins*; Lever, A. B. P., Gray, H. B., Eds.; Addison-Wesley: Reading, MA, 1983; Vol. II. Li, X. Y. Spiro, T. G. *J. Am. Chem. Soc.* **1988**, *110*, 6024.

(37) Hill, Jeffrey R.; Dlott, D. D.; Fayer, M. D.; Peterson, K. A.; Rella, C. W.; Rosenblatt, M. M.; Suslick, K. S.; Ziegler, C. J. *Chem. Phys. Lett.* **1995**, *244*, 218.

(38) Hill, J. R.; Tokmakoff, A.; Peterson, K. A.; Sauter, B.; Zimdars, D. A.; Dlott, D. D.; Fayer, M. D. *J. Phys. Chem.* **1994**, *98*, 11213. Hill, J. R.; Dlott, D. D.; Rella, C. W.; Peterson, K. A.; Decatur, S. M.; Boxer, S. G.; Fayer, M. D. *J. Phys. Chem.* **1996**, accepted. Hill, J. R.; Dlott, D. D.; Rella, C. W.; Smith, T. I.; Schwettman, H. A.; Peterson, K. A.; Kwok, A.; Rector, K.; Fayer, M. D. *Biospec.* **1996**, submitted for publication. Hill, J. R.; Dlott, D. D.; Fayer, M. D.; Rella, C. W.; Rosenblatt, M. M.; Suslick, K. S.; Ziegler, C. J. *J. Phys. Chem.* **1996**, accepted for publication.

JP961129R